JACS
JOURNAL OF THE AMERICAN CHEMICAL SOCIETY
Article
pubs.acs.org/JACS

Orthogonal Self-Assembly in Folding Block Copolymers

Nobuhiko Hosono,[†] Martijn A. J. Gillissen,[†] Yuanchao Li,[‡] Sergei S. Sheiko,[‡] Anja R. A. Palmans,*[,†] and E. W. Meijer*[,†]

[†]Institute for Complex Molecular Systems, Laboratory of Macromolecular and Organic Chemistry, Eindhoven University of Technology, P.O. Box 513, 5600 MB Eindhoven, The Netherlands

[‡]Department of Chemistry, University of North Carolina at Chapel Hill, Chapel Hill, North Carolina 27599-3290, United States

Supporting Information

ABSTRACT: We herein report the synthesis and characterization of ABA triblock copolymers that contain two complementary association motifs and fold into single-chain polymeric nanoparticles (SCPNs) via orthogonal self-assembly. The copolymers were prepared using atom-transfer radical polymerization (ATRP) and possess different pendant functional groups in the A and B blocks (alcohols in the A block and acetylenes in the B block). After postfunctionalization, the A block contains *o*-nitrobenzyl-protected 2-ureidopyrimidinone (UPy) moieties and the B block benzene-1,3,5-tricarboxamide (BTA) moieties. While the protected UPy groups dimerize after photoinduced deprotection of the *o*-nitrobenzyl group, the BTA moieties self-assemble into helical aggregates when temperature is reduced. In a two-step thermal/photoirradiation treatment under dilute conditions, the ABA block copolymer forms both BTA-based helical aggregates and UPy dimers intramolecularly. The sequential association of the two self-assembling motifs results in single-chain folding of the polymer, affording nanometer-sized particles with a compartmentalized interior. Variable-temperature NMR studies showed that the BTA and UPy self-assembly steps take place orthogonally (i.e., without mutual interference) in dilute solution. In addition, monitoring of the intramolecular self-assembly of BTA moieties into helical aggregates by circular dichroism spectroscopy showed that the stability of the aggregates is almost independent of UPy dimerization. Size-exclusion chromatography (SEC) and small-angle X-ray scattering analysis provided evidence of significant reductions in the hydrodynamic volume and radius of gyration, respectively, after photoinduced deprotection of the UPy groups; a 30−60% reduction in the size of the polymer chains was observed using SEC in $CHCl_3$. Molecular imaging by atomic force microscopy (AFM) corroborated significant contraction of individual polymer chains due to intramolecular association of the BTA and UPy groups. The stepwise folding process resulting from orthogonal self-assembly-induced supramolecular interactions yields compartmentalized SCPNs comprised of distinct microdomains that mimick two secondary-structuring elements in proteins.

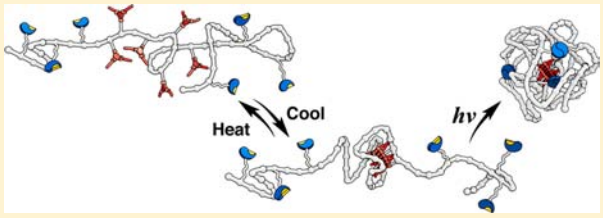

INTRODUCTION

Protein folding is a dynamic process of molecular self-assembly during which a single-stranded polypeptide chain folds to form a well-defined three-dimensional (3D) tertiary structure.[1] One of the defining features of this tertiary structure is the presence of individually folded domains (α-helixes, β-sheets), which enable these biomacromolecules to fulfill dedicated functions in catalysis, recognition, and signaling.[2] Enzymes, for example, have evolved to take full advantage of their 3D structures in order to realize remarkable catalytic activities and selectivities by encapsulating multiple recognition sites close to the catalytically active center within compartmentalized domains.[3] To fix this unique, active conformation with high fidelity, nature applies a dynamic and reversible folding mechanism that relies to a large extent on non-covalent interactions.[4]

Inspired by nature's way, several approaches for preparing synthetic analogues of folded proteins using, for example, helical polymers[5] and dendrimers[6] have been explored. In addition, a number of systems have been reported in which synthetic polymers were collapsed through covalent bond formation[7] or supramolecular associations[8] to achieve a compartmentalized structure.[9] We recently developed single-chain folding of synthetic polymers bearing a single self-assembling motif. Either benzene-1,3,5-tricarboxamide (BTA)[10] or 2-ureido-4[1*H*]-pyrimidinone (UPy)[11] moieties were applied as the recognition motif to induce single-chain folding under selected conditions. BTA is a well-explored helically self-assembling motif that forms aggregates through threefold-symmetric hydrogen bonding.[12] The UPy motif forms a dimer complex with a large equilibrium constant through complementary quadruple hydrogen bonding.[13] When incorporated into synthetic macromolecules, each of these self-assembling motifs leads to controlled single-chain folding.

In contrast to biological systems, where orthogonal self-assembly is one of the essential features for the formation of tertiary structures,[1,4] examples of multiple orthogonal self-assembling motifs in folding of synthetic macromolecules are

Received: October 22, 2012
Published: November 26, 2012

   dx.doi.org/10.1021/ja310422w | *J. Am. Chem. Soc.* 2013, 135, 501−510

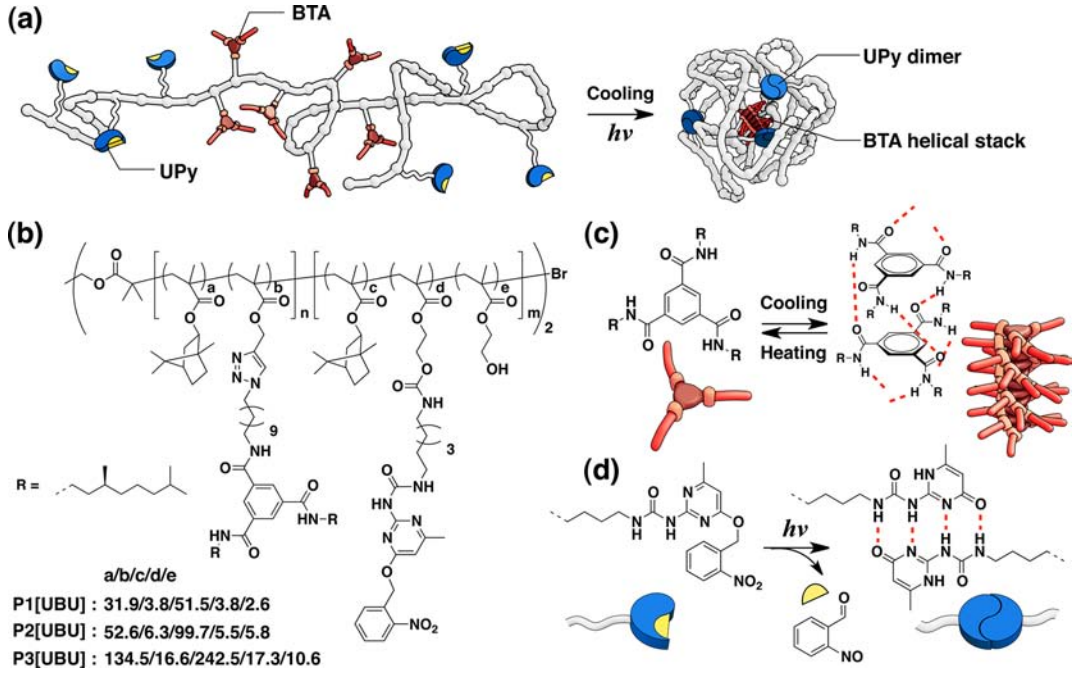

Figure 1. (a) Design of a triblock copolymer with BTA and UPy moieties that folds into a single-chain polymeric nanoparticle cross-linked via orthogonal self-assembly. (b) Chemical structure of the triblock copolymers **P1**[**UBU**], **P2**[**UBU**], and **P3**[**UBU**]. (c) Helical self-assembly of chiral BTAs via threefold-symmetric hydrogen bonding. (d) Photoinduced dimerization of *o*-nitrobenzyl-protected UPys via quadruple hydrogen bonding.

very rare. The only example reported to date describes the self-folding of a polymer chain initiated by two pairwise hydrogen-bonding interactions that self-assemble orthogonally.[8e] Quite recently, we and others have applied the concept of orthogonal self-assembly to design novel materials.[14,15] For example, materials using self-assembly of BTA and UPy motifs were prepared in which the two motifs individually form phase-segregated nanorods in an orthogonal fashion, affording cross-linked polymeric materials.[15] A molecular design approach combining both of these self-assembling motifs in a folding block copolymer would represent a significant milestone leading to synthetic protein analogues in which orthogonal self-assembly would induce folding of each block into internal segregated domains. In fact, such a system would exhibit the conformational adaptability and perfectly organized inner structure of proteins, both of which are essential for their effective functioning.

We herein report the synthesis and characterization of a series of ABA triblock copolymers that fold into single-chain polymeric nanoparticles (SCPNs) by intramolecular orthogonal self-assembly (Figure 1). The compartmentalized architectures were successfully realized by incorporating BTA and UPy motifs into the B and A blocks, respectively. The use of a photocleavable protecting group on the UPy moiety enabled a two-step folding process triggered by a temperature decrease for BTA self-assembly and light irradiation for UPy dimerization. During the folding process, the selected motifs organized into individual helical and dimeric aggregates through mutual recognition properties, resulting in a compartmentalized structure. The folding process was fully characterized using a combination of ^{1}H NMR and circular dichroism (CD) spectroscopy, size-exclusion chromatography (SEC), and small-angle X-ray scattering (SAXS). In addition, atomic force microscopy (AFM) was used to monitor the folding process on the molecular scale and provided a clear view of the single-molecule nanostructures.

RESULTS AND DISCUSSION

Polymer Design. We designed the ABA triblock copolymers **P1**[**UBU**], **P2**[**UBU**], and **P3**[**UBU**] having chiral BTA moieties in the middle (B) block and UPy moieties in both end (A) blocks (Figure 1). A postpolymerization functionalization approach was employed to introduce the BTA and UPy motifs, which reduced the synthetic effort.[16] Because of its tolerance toward a variety of functional groups, we used Cu(I)-catalyzed atom-transfer radical polymerization (ATRP)[17] to copolymerize the postfunctionalizable monomers propargyl methacrylate (PMA) and hydroxyethyl methacrylate (HEMA) with isobornyl methacrylate (IBMA). We first prepared the polymeric scaffolds bearing postfunctionalizable alkyne and hydroxyl groups (the so-called "bare" block copolymers), poly(IBMA-*co*-HEMA)-*block*-poly(IBMA-*co*-PMA)-*block*-poly(IBMA-*co*-HEMA), denoted as **P***n*[−−−] (*n* = 1−3) (see Scheme 1). IBMA was chosen as the comonomer to enhance the solubility of the resulting polymers. Reaction of **P***n*[−−−] with azide-substituted BTA **2**[10a] through Cu(I)-catalyzed azide−alkyne cycloaddition (CuAAC) afforded the BTA-functionalized polymers, denoted as **P***n*[−**B**−]. Subsequent reaction of **P***n*[−**B**−] with isocyanate-functionalized, *o*-nitrobenzyl-protected UPy **3**[11d] resulted in the desired triblock copolymers, denoted as **P***n*[**UBU**]. This approach allowed for convenient double functionalization of the copolymers with both BTA and UPy moieties.

The use of a photocleavable protecting *o*-nitrobenzyl group allowed us to trigger the folding processes in a stepwise fashion. While the BTA moiety undergoes internal helical stack formation in a cooperative manner, a process that is sensitive to temperature,[10] irradiation with UV light under diluted conditions results in UPy dimer formation. We selected this stepwise approach because it is reminiscent of the folding of proteins, in which different secondary structures are first formed and then the 3D structure is attained.[1] In our case, we

dx.doi.org/10.1021/ja310422w | *J. Am. Chem. Soc.* 2013, 135, 501−510

Scheme 1. Synthesis of Folding Triblock Copolymers Using a Postfunctionalization Approach

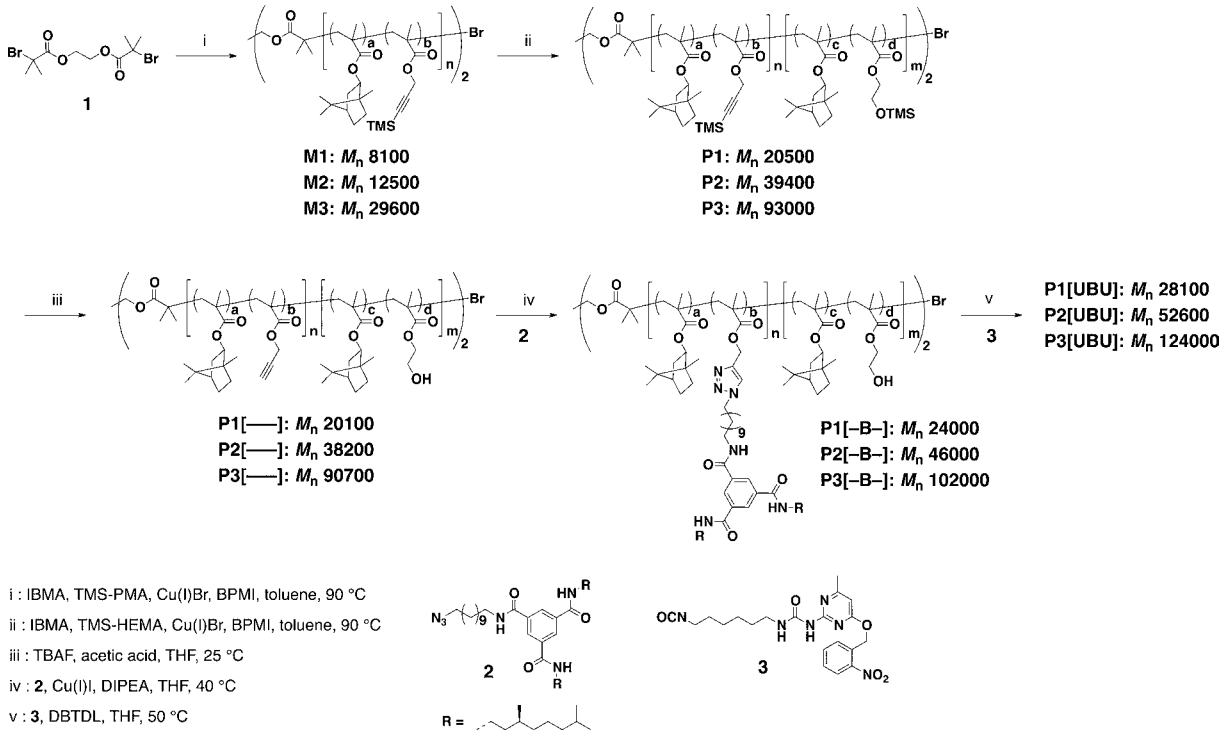

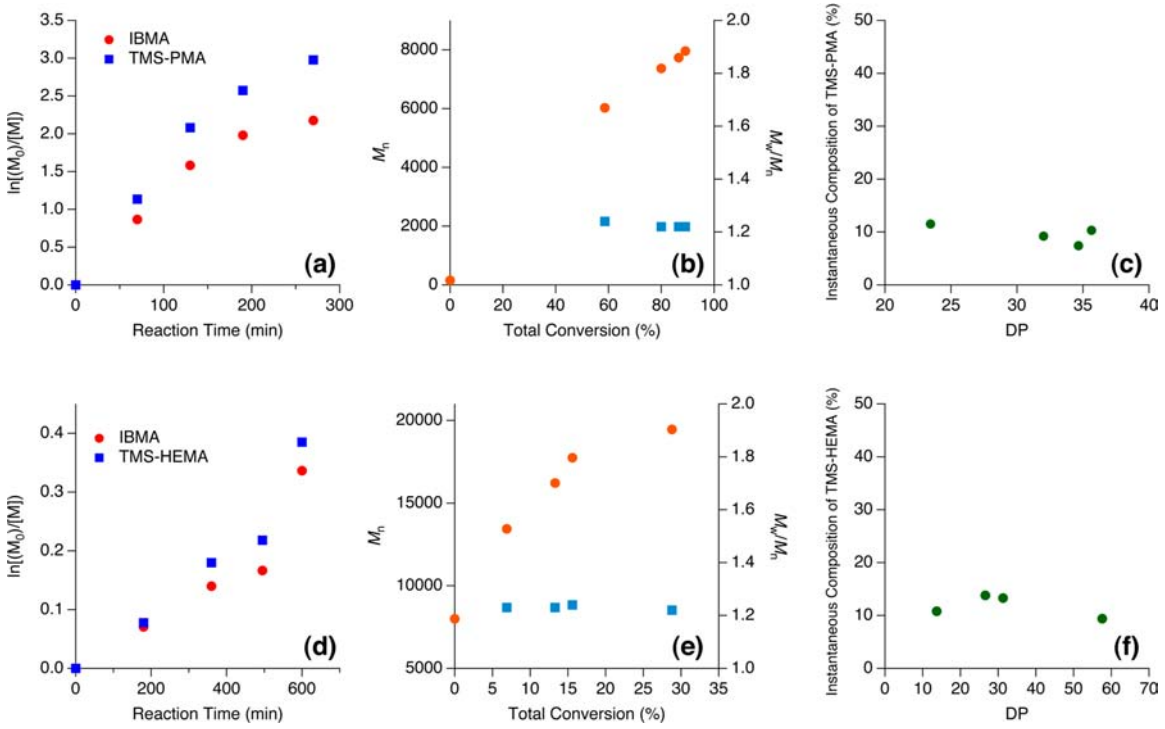

Figure 2. (a, d) Kinetic plots for the copolymerizations of (a) IBMA and TMS-PMA for **M1** and (d) IBMA and TMS-HEMA for **P1** by ATRP in the presence of a CuBr/BPMI catalyst. (b, e) Dependence of M_n and PDI on the total monomer conversion for the copolymerizations of (b) IBMA and TMS-PMA for **M1** and (e) IBMA and TMS-HEMA for **P1**. (c, f) Instantaneous compositions of (c) TMS-PMA for **M1** and (f) TMS-HEMA for **P1** as functions of the degree of polymerization.

anticipated that sequential cooling and UV irradiation would afford triblock copolymers folded into compartmentalized SCPNs in a controlled manner through orthogonal self-assembly. Both BTA and UPy self-assembly were probed by NMR spectroscopy, and BTA self-assembly could also be monitored by CD spectroscopy. In addition, the chain collapse was quantified by SEC and synchrotron-radiation SAXS (SR-SAXS).

Synthesis of Triblock Copolymers Bearing Both BTA and UPy Motifs. The postfunctionalizable "bare" polymers

dx.doi.org/10.1021/ja310422w | J. Am. Chem. Soc. 2013, 135, 501–510

with acetylene groups in the B block and hydroxyl groups in both A blocks were readily prepared by two-step ATRP[17] (Scheme 1). Starting from bifunctional initiator **1**, the B block consisting of poly(IBMA-*co*-TMS-PMA) was polymerized first, and then the two A blocks consisting of poly(IBMA-*co*-TMS-HEMA) were grown from the resulting macroinitiator. Initiator **1** is commercially available and has no absorption at the irradiation wavelength required for the *o*-nitrobenzyl deprotection. The trimethylsilyl (TMS)-protected monomers TMS-PMA[18] and TMS-HEMA[19] were used to avoid undesirable interactions with and coordination to the catalyst, since it has been reported that the unprotected monomers may give rather broad polydispersity indices (PDI = M_w/M_n, where M_w and M_n are the weight-average and number-average molecular weights, respectively), especially in the case of PMA.[18a] In the present study, the monomer feed ratio of each functionalized monomer with respect to IBMA was fixed at 10% in both blocks. Toluene was used as the reaction solvent, and the monomer conversion was followed by gas chromatography (GC) using *p*-xylene as an internal standard. To investigate the influence of the molecular weight of the triblock copolymer on the folding properties, we aimed for three different polymers, **P1**−**P3**, with degrees of polymerization (DPs) ranging from 90 to 420.

For the synthesis of the **P1** series, we first prepared the macroinitiator **M1**. Copolymerization of TMS-PMA and IBMA in the presence of a CuBr/*N*-butyl-2-pyridylmethanimine (BPMI) catalyst[20] showed good control, as evidenced by the kinetic plots (Figure 2a,b). The polymerization proceeded with a small termination reaction and a slight difference in the reaction rates for the two monomers, with TMS-PMA being slightly more reactive than IBMA (Figure 2a). From the monomer conversion data, we calculated the instantaneous composition of TMS-PMA along with the DP (Figure 2c), since the incorporation sequence of the acetylene-functionalized monomers ultimately determines the secondary structure of the polymer. The sequence was expected to be crucial for the self-assembling event, which strongly depends on the local concentration of self-assembling motifs. The calculation was carried out following the work of Matyjaszewski and co-workers on spontaneous gradient copolymerization for brush polymers.[21] From the monomer feed ratio, the instantaneous composition of acetylene-functionalized monomers in the polymer backbone was calculated to be 10% in any part of polymer. Gratifyingly, the calculated instantaneous composition of TMS-PMA showed a constant value of ∼10% at all DPs. At 90% conversion, the reaction mixture was exposed to air and diluted in tetrahydrofuran (THF). The resultant polymer was precipitated from methanol, affording macroinitiator **M1**, poly(IBMA-*co*-TMS-PMA) (M_n = 8100 g/mol), as a white powder (Scheme 1).

In the next step, the copolymerization of TMS-HEMA and IBMA started with the macroinitiator **M1**. Analysis of Figure 2d,e indicates that also in this case good control was obtained. The calculated instantaneous composition of TMS-HEMA maintained a constant value of ∼10% at all DPs (Figure 2f), showing that obtaining **P1** with good control over the copolymer composition (M_n = 20 500 g/mol, PDI ≈ 1.2) is feasible with different functional groups in the A and B blocks. Subsequent removal of the TMS groups using tetrabutylammonium fluoride (TBAF) afforded the bare triblock copolymer **P1**[−−−] (M_n = 20 100 g/mol) bearing acetylene and hydroxyl groups in the B and A blocks, respectively. By a similar approach, the other two bare polymers with different molecular weights, **P2**[−−−] and **P3**[−−−] (M_n = 38 200 and 90700 g/mol, respectively; Scheme 1), were prepared. All of the data for the numbers of incorporated functional groups of both types are summarized in Table 1.

Table 1. Conditions and Results for the Triblock Copolymerizations by ATRP

			M_n (g/mol)			
polymer	initiator	monomers	calcd[c]	exptl[d]	PDI	$n_{C\equiv C}/n_{OH}$[e]
M1	**1**	IBMA /TMS-PMA[a]	7800	8100	1.21	3.8/−
M2	**1**	IBMA/TMS-PMA[a]	12900	12500	1.21	6.3/−
M3	**1**	IBMA/TMS-PMA[a]	33100	29600	1.20	16.6/−
P1	**M1**	IBMA/TMS-HEMA[a]	20500	20500	1.24	3.8/6.4
P2	**M2**	IBMA/TMS-HEMA[b]	37400	39400	1.33	6.3/11.3
P3	**M3**	IBMA/TMS-HEMA[b]	89200	93000	1.54[f]	16.6/27.9

[a]ATRP was carried out with $[CuBr]_0:[I]_0:[BPMI]_0$ = 2:1:4, where I is the initiator. The ratio of IBMA to functionalized monomer (TMS-PMA or TMS-HEMA) was 9:1. [b]Same as *a*, except that $[CuBr]_0:[I]_0:[BPMI]_0$ = 4:1:8. For details, see the Supporting Information. [c]Calculated as $[MW_I + ([M_1]_0/[I]_0) \times MW_1 \times conv_1 + ([M_2]_0/[I]_0) \times MW_2 \times conv_2]$, where MW_I is the molecular weight of the initiator, MW_i and $conv_i$ are the molecular weight and conversion, respectively, of monomer M_i (i = 1: IBMA; i = 2: TMS-PMA or TMS-HEMA). [d]Determined via SEC using THF as the eluent, calibrated with polystyrene standards. [e]$n_{C\equiv C}$ and n_{OH} are the numbers of acetylene and hydroxyl groups per chain, respectively, as calculated from the conversions of the functionalized monomers. [f]The molecular weight distribution was bimodal.

Subsequently, the pendant acetylene and hydroxyl groups were functionalized with azide-functionalized BTA **2** and protected UPy **3**, respectively, affording the desired triblock copolymers bearing both self-assembling motifs, **P1**[**UBU**], **P2**[**UBU**], and **P3**[**UBU**] (28 100, 52 600, and 124 000 g/mol, respectively; Scheme 1). The numbers of incorporated BTA and protected UPy moieties in the polymers were determined by a combination of ^{1}H NMR and ATRP conversion data. The results for polymers **P1**−**P3** are summarized in Table 2. First, the CuAAC reactions with **2** were performed in deoxygenated THF in the presence of the stoichiometric Cu(I) catalyst generated in situ from CuI and *N*,*N*-diisopropylethylamine (DIPEA), which afforded the **P***n*[−**B**−] series of polymers bearing only BTA moieties on the B block. The **P***n*[−**B**−] polymers were then reacted with **3** using dibutyltin dilaurate (DBTDL) as a catalyst. The reaction mixtures were precipitated from hexane and then methanol twice, affording the double-functionalized **P***n*[**UBU**] series of polymers. As an example, Figure 3 shows the representative SEC traces for the **P1** series. Side reactions and undesired associations were not observed during the postfunctionalization reactions.

Orthogonal Self-Assembly Followed by NMR Spectroscopy. In the past, variable-temperature NMR (VT-NMR) spectroscopy has been shown to be a powerful technique to assess the orthogonality of different self-assembling systems.[9f,14e] Thus, we performed VT-NMR analysis of **P2**[**UBU**] before and after irradiation (Figure 4). Figure 4a depicts the temperature-dependent NMR spectra of **P2**[**UBU**] in pure d_4-dichloroethane (d_4-DCE) at 1.0 mg/mL concentration before

dx.doi.org/10.1021/ja310422w | J. Am. Chem. Soc. 2013, 135, 501−510

Table 2. Data for the Triblock Copolymer Synthesis

	M_n (g/mol) (PDI)[a] [n_F][b]		
	[−−−]	[−B−]	[UBU]
P1	20100 (1.25) [$3.8_{C\equiv C}$] [6.4_{OH}]	24000 (1.17) [3.8_{BTA}] [6.4_{OH}]	28100 (1.16) [3.8_{BTA}] [$3.8_{UPy}/2.6_{OH}$]
P2	38200 (1.34) [$6.3_{C\equiv C}$] [11.3_{OH}]	46000 (1.30) [6.3_{BTA}] [11.3_{OH}]	52600 (1.26) [6.3_{BTA}] [$5.5_{UPy}/5.8_{OH}$]
P3	90700 (1.53) [$16.6_{C\equiv C}$] [27.9_{OH}]	102000 (1.48) [16.6_{BTA}] [27.9_{OH}]	124000 (1.46) [16.6_{BTA}] [$17.3_{UPy}/10.6_{OH}$]

[a]Determined via SEC using THF as the eluent, calibrated with polystyrene standards. [b]Numbers of incorporated functional groups (indicated by the subscripts), determined via ^{1}H NMR with reference to the corresponding numbers determined previously.

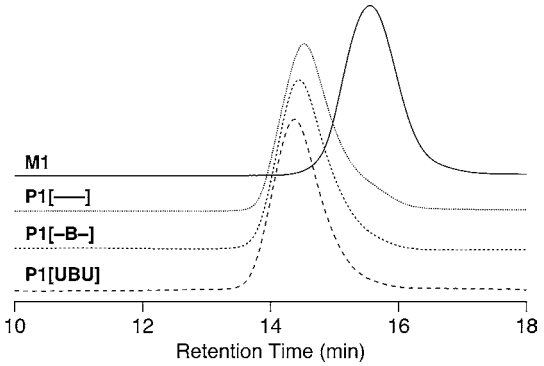

Figure 3. SEC traces of **M1**, **P1**[−−−], **P1**[−B−], and **P1**[**UBU**] recorded with a refractive index detector using THF as the eluent.

UV irradiation. A pronounced peak shift and broadening of the protons attributed to the BTA moieties were clearly observed upon cooling from 80 to 20 °C. The broadening of the signals is indicative of BTA self-assembly. The peak at 6.6 ppm, corresponding to the amide protons on the BTA moieties, shifted downfield upon cooling, indicative of threefold hydrogen-bond formation by BTAs.[22] After 350 nm UV light irradiation of the sample at 20 °C, the spectra showed that a peak originating from benzyl protons on the protected UPy moieties disappeared and other peaks corresponding to UPy dimers simultaneously appeared at 10.1, 11.8, and 13.1 ppm (Figure S1 in the Supporting Information).[13d] At the same time, the BTA peaks remained broad, indicating that their self-assembly was not affected. The deprotection was completed after 20 min irradiation. These results suggest that both motifs were self-assembled under the conditions applied.

After completion of the deprotection, we heated the sample to 80 °C again and recorded NMR spectra as the sample was cooled to 20 °C (Figure 4b). At higher temperature, the BTA proton signals sharpened, and the UPy dimer protons broadened and disappeared above 50 °C, indicating that all of the hydrogen bonds were broken. Under these conditions, the polymer unfolded and adopted a random coil conformation. Upon cooling, the BTA signals showed the expected broadening and downfield shifts, and the UPy dimer signals reappeared. Importantly, the behavior of the BTAs was identical in the presence and absence of UPy dimers. This indicates that the hydrogen bonds between the different supramolecular motifs were restored and that the self-assembly was orthogonal (i.e. the two self-assembly events occurred independently of each other). As a result, a folded structure comprising compartments stabilized by UPy dimers and compartments stabilized by BTA helical aggregates was formed.

Intramolecular BTA Self-Assembly Followed by CD Spectroscopy. The self-assembly of chiral BTA moieties on the B block of the polymer was investigated with temperature-dependent CD spectroscopy (Figure 5). We selected the mixed solvent system of methylcyclohexane (MCH) and 1,2-DCE (25/75 v/v). For hydrogen-bonding-induced polymer folding, one has to consider the critical balance between backbone solubility and self-assembly capability of the hydrogen-bonding motif, which prefers less polar solvents. Previously, we discussed the importance of solvent polarity on BTA-driven SCPN formation.[10] "Free" BTAs self-assemble in apolar solvents such as dodecane, heptane, and MCH.[12] When attached to a polymer, however, two conflicting propensities, aggregation of BTAs and solvation of the polymer backbone, have to be balanced by the solvent polarity and temperature in order to obtain SCPNs. Increasing the solvent polarity or solution temperature brings about unfolding (denaturation) of the SCPNs. The 25/75 (v/v) MCH/DCE mixture provides a compromise between BTA aggregation and polymer solubility, allowing us to follow the whole folding process in a convenient temperature window between 80 and 20 °C.

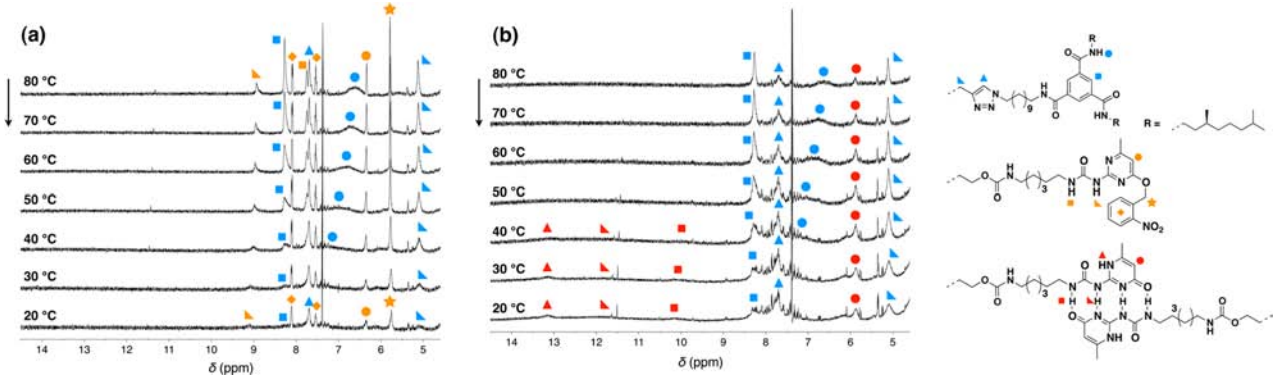

Figure 4. Arrays of VT-NMR spectra recorded for 1 mg/mL solutions in d_4-DCE upon cooling from 80 to 20 °C for **P2**[**UBU**] (a) before and (b) after UV irradiation (**P2**[**UBU**]**UV**). The solvent peak was used as an internal standard. The insets depict the assignments of protons on BTA (blue), protected UPy (yellow), and the UPy dimer complex (red).

dx.doi.org/10.1021/ja310422w | J. Am. Chem. Soc. 2013, 135, 501−510

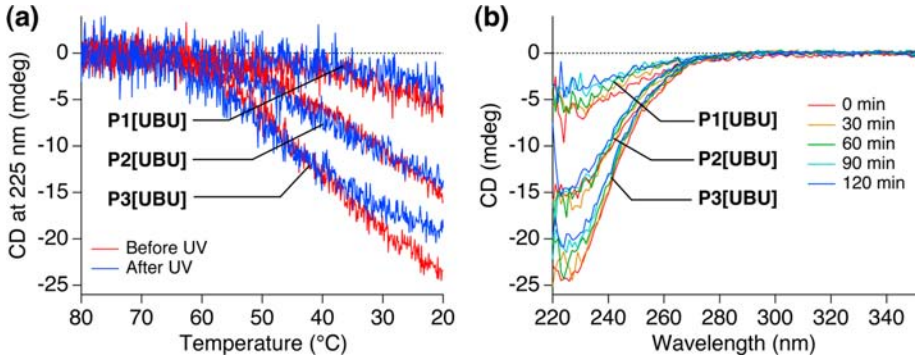

Figure 5. (a) CD cooling curves of **P1**[**UBU**], **P2**[**UBU**], and **P3**[**UBU**] before (red) and after (blue) UV irradiation (c_{BTA} = 50 μM) monitored at λ = 225 nm in 25/75 (v/v) MCH/DCE at temperatures from 80 to 20 °C (cooling rate 1 °C/min). (b) CD spectra of **P1**[**UBU**], **P2**[**UBU**], and **P3**[**UBU**] in 25/75 (v/v) MCH/DCE at 20 °C during 120 min of 350 nm UV irradiation.

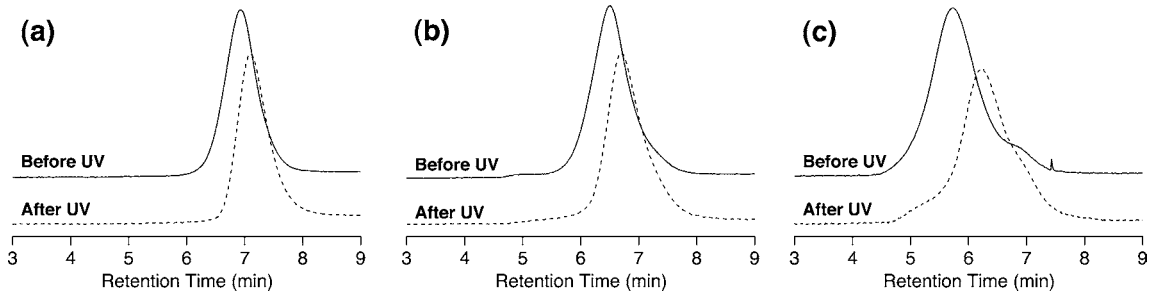

Figure 6. SEC traces for (a) **P1**[**UBU**], (b) **P2**[**UBU**], and (c) **P3**[**UBU**] before and after 2 h of 350 nm UV irradiation, recorded with a UV detector using $CHCl_3$ as the eluent.

The CD spectra of the three triblock copolymers carrying both BTA and protected UPy were measured on cooling from 80 to 20 °C (Figure 5a). The BTA concentration (c_{BTA}) was fixed at 50 μM in all polymer solutions. To ensure that self-assembly would be under thermodynamic control, slow cooling (1 °C/min) was applied. Above 65 °C, all of the polymers were CD-silent, indicating that the polymers were molecularly dissolved and adopted fully unfolded conformations. Upon cooling, a negative Cotton effect was observed for all of the polymers with a maximum at λ = 225 nm, in agreement with our previous reports and indicative of the formation of left-handed helical columnar aggregates inside the polymer.[10,12]

The CD signal intensity of these three polymer solutions was proportional to the number of BTAs per chain when the molar concentrations of BTA units were identical. This shows that the BTA self-assembly event occurs within a single chain (Figure 5). These observations are all consistent with our previous work on BTA-based SCPNs, in which we found that the local BTA concentration is responsible for the magnitude of the Cotton effect.[10] Taking these results into account, we propose that before UV irradiation, the block copolymers are partially folded as a result of intramolecular BTA self-assembly in the middle block.

Subsequent UV irradiation provided the polymers **P1**[**UBU**]**UV**, **P2**[**UBU**]**UV**, and **P3**[**UBU**]**UV**, in which the UPy groups were deprotected and formed dimers (see above). The CD spectra at 20 °C before and after irradiation (Figure 5b) were identical, confirming the NMR results that UPy dimer formation did not interfere with the BTA self-assembly. The stability of the BTA aggregates was investigated by heating and cooling the samples and probing the CD effect as a function of temperature at 225 nm. The cooling curves before and after UV irradiation were superimposable, indicating that UPy dimerization did not affect the stability of the BTA helical aggregates. Only the largest polymer, **P3**[**UBU**]**UV**, showed a small deviation in the CD cooling curve from that obtained before irradiation. The decrease in CD signal could have been caused by the fact that the BTA columnar aggregates were disrupted as a result of large conformational changes of the polymer arising from intramolecular UPy association. Alternatively, there may have been some loss of the orthogonality between the BTA and UPy self-assembly processes due to high incorporation of both groups in the single polymer. Importantly also, in pure DCE as the solvent, in which "free" BTAs are molecularly dissolved under these conditions, all of the polymers showed CD signals similar in shape albeit with reduced intensity compared with those observed in the 25/75 (v/v) MCH/DCE mixed solvent. In pure DCE, **P2**[**UBU**]**UV** also exhibited a small deviation in the intensity of the CD signal after UV irradiation, while it did not in the 25/75 (v/v) MCH/DCE mixed solvent (Figure S2 in the Supporting Information). These observations suggest that the degree of orthogonality also depends on the balance between the backbone solubility and the self-assembly capability of the hydrogen-bonding motif.

Chain Collapse Induced by Intramolecular UPy Association. While NMR and CD spectroscopy are useful for gathering information on the orthogonality of the self-assembling motifs, they do not provide information on the effect of self-assembly on the polymer conformation. For this purpose, we used SEC and SR-SAXS analyses. Both techniques provide information on the volume of the polymer coil, which can be related to the degree to which the polymer adopts a random coil conformation or is present in a collapsed state. After UV light irradiation, the triblock copolymers were analyzed by SEC measurements in chloroform and THF (Figure 6 and Table 3). The SEC samples were prepared by

dx.doi.org/10.1021/ja310422w | J. Am. Chem. Soc. 2013, 135, 501−510

Table 3. SEC Data for the Triblock Copolymers and Photoinduced Intramolecular Collapse[a]

	$CHCl_3$ SEC[b]					THF SEC[c]				
	before irradiation		after irradiation for 2 h			before irradiation		after irradiation for 2 h		
polymer	M_n (g/mol)	PDI	M_n (g/mol)	PDI	% decrease	M_n (g/mol)	PDI	M_n (g/mol)	PDI	% decrease
P1[**UBU**]	27000	1.35	17800	1.29	34	28100	1.16	26000	1.18	7.4
P2[**UBU**]	50600	1.65	32500	1.91	36	52600	1.26	43900	1.33	17
P3[**UBU**]	158000	2.60	60700	2.60	62	124000	1.46	100200	1.57	19

[a]Reaction conditions: polymer (0.5 mg/mL) dissolved in 25/75 (v/v) MCH/DCE mixed solvent was exposed to 350 nm UV irradiation for 2 h and then subjected to SEC analysis without further treatment. [b]Determined via SEC using $CHCl_3$ as the eluent, calibrated with polystyrene standards. [c]Determined via SEC using THF as the eluent, calibrated with polystyrene standards.

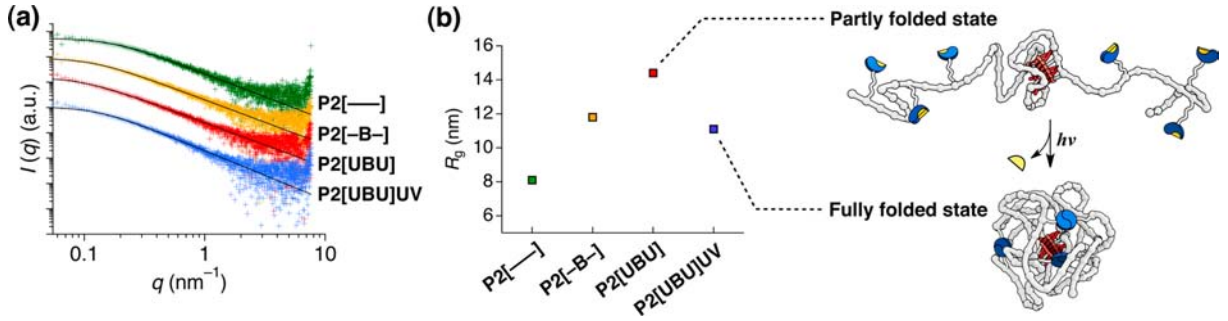

Figure 7. (a) SAXS data and fitting curves (black solid lines) of **P2**[−−−], **P2**[−**B**−], **P2**[**UBU**], and **P2**[**UBU**] after UV irradiation. The SAXS data were recorded in 1 mg/mL solutions in 75/25 (v/v) MCH/1,4-dioxane at 20 °C and are drawn here on the same scale but offset vertically for clarity. (b) R_g values for **P2**[−−−], **P2**[−**B**−], **P2**[**UBU**], and **P2**[**UBU**]**UV** obtained from fitting analysis of the SAXS data. The insets schematically illustrate the triblock copolymer in a partly folded state and the fully folded state after UV irradiation.

dissolving the protected polymers in the 25/75 (v/v) MCH/DCE mixed solvent at 0.5 mg/mL concentration and then irradiating them with 350 nm UV light for 2 h. The irradiated solutions were subjected to SEC directly without any further treatment. The volume decrease of the polymer coil was a result of intramolecular UPy dimerization after the cleavage of protecting group, leading to a collapse of the polymer chain.[11] The chain collapse was large (34−62%) when chloroform was used as the eluent (Figure 6). On the other hand, SEC using THF as the eluent showed a rather small volume change for all of the polymers, although the extent of the volume decrease was similar to that for UPy-pendant SCPNs (18%−22% for a PMMA backbone with 10% UPy incorporation) reported in our previous work using THF as a SEC eluent.[11c] Because **P2**[**UBU**] showed a CD signal in pure DCE but not in pure THF, the eluent dependence of the volume decrease might have been related to BTA self-assembly on the polymer. Intriguingly, the largest polymer, **P3**[**UBU**], showed an extraordinarily large volume decrease of 62% in $CHCl_3$ SEC measurements. This result is quite consistent with the CD signal decrease of **P3**[**UBU**] observed upon UPy deprotection and gives reasonable explanation for the hypothesis that such a large collapse may disrupt internal BTA helical stacks. With the large shift of the main SEC peak toward low-molecular-weight region, a small shoulder at higher molecular weight could be observed (Figure 6). This tendency became more pronounced in higher-DP polymers, indicating the presence of some intermolecular UPy association. In fact, we found that the distinct shoulder became much larger when the samples were prepared at higher concentrations of 1.0 mg/mL (Figure S3 in the Supporting Information).[23] Thus, these observations are certainly indicative of the intermolecular polymer interactions, which increase with the volume concentrations of polymers.

SR-SAXS measurements were done with the **P2** polymer series of [−−−], [−**B**−], [**UBU**], and [**UBU**]**UV** in 75/25 (v/v) MCH/1,4-dioxane (Figure 7). Because chlorinated solvents absorb a large part of the X-ray radiation, preventing useful measurements, we changed from DCE to 1,4-dioxane. Even in 75/25 (v/v) MCH/1,4-dioxane, the BTA moieties on the polymer self-assembled into helical columnar aggregates and gave a typical CD signal (Figure S4 in the Supporting Information). Fitting of the SAXS curves provided the radius of gyration (R_g) and the excluded volume parameter (ν) of the polymers before and after irradiation.[23] The bare polymer **P2**[−−−] showed R_g = 8.1 ± 0.1 nm (ν = 0.547 ± 0.004), and the corresponding functionalized polymers **P2**[−**B**−] and **P2**[**UBU**] showed R_g = 11.8 ± 0.3 nm (ν = 0.561 ± 0.004) and 14.4 ± 0.3 nm (ν = 0.567 ± 0.003), respectively (Figure 7b). The increase in R_g is consistent with an increase in the mass of the polymers upon functionalization.

UV irradiation of **P2**[**UBU**] to produce **P2**[**UBU**]**UV** resulted in a significant decrease in R_g to 11.1 ± 0.2 nm (ν = 0.513 ± 0.003), corresponding to a size reduction of 22.9%. The decrease in R_g is in good agreement with the calculated value of 19.8% obtained from the M_n decrease in SEC analysis with an assumption of $R_g \sim M_n^{\nu} \sim M_n^{0.5}$.[24] The ν value for **P2**[**UBU**] also showed a decrease after UV irradiation, indicating that the polymer adopts more compact conformation as a result of the strong dimerization between UPys incorporated at the two ends of the polymer. These observations provide a clear image of the fully folded state whereby the triblock copolymer adopts a globular shape with both internal helical and dimeric structures (Figure 7).

Microstructure of Individual SCPNs Imaged by AFM. AFM is a powerful tool for imaging the nanostructures of individual macromolecules[25] and polymeric nanoparticles[11] on surfaces. Since the second folding process induced by

dx.doi.org/10.1021/ja310422w | J. Am. Chem. Soc. 2013, 135, 501−510

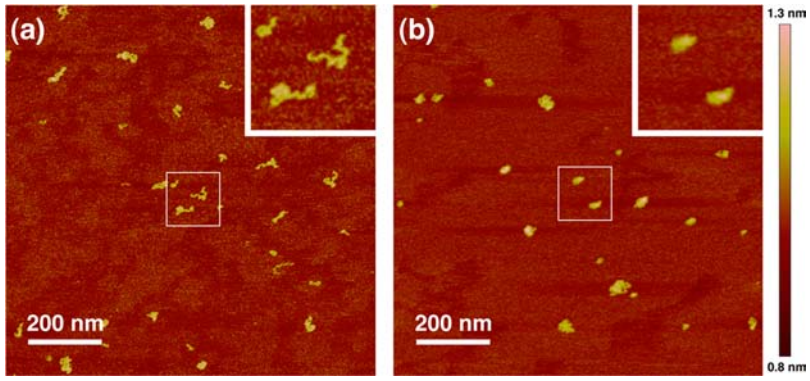

Figure 8. AFM height images of **P3**[**UBU**] capture two-steps of the molecular folding process (a) before and (b) after UV irradiation. The film samples were prepared by spin-casting from diluted DCE solution on a mica substrate. The top-right insets show magnifications of the framed areas.

photoinduced UPy association in **P3**[**UBU**] is related to a significant volume reduction, we anticipated that changes in the polymer conformation before and after deprotection could be readily followed by AFM. Thus, we prepared two thin-film samples of **P3**[**UBU**] before and after UV irradiation by spin-casting a highly diluted DCE solution (0.05 μg/mL) on mica substrates.[23] In both cases, AFM measurements showed the presence of individual block copolymers (Figure 8a,b and Figures S5 and S6 in the Supporting Information). Before UV irradiation, some individual chains adopted a "bead−tail" conformation. Their visual appearance is highly reminiscent of the "partly folded" state (Figures 8a and 7b), in which only BTA moieties in the middle block self-assemble into internal helical stacks and partly collapse the polymer chain. Subsequently, UV irradiation triggered intramolecular UPy association resulting in complete collapse of individual polymer chains into nanoparticles. The AFM images, clearly depict this drastic chain collapse and image the "fully folded" SCPNs (Figure 8b). Apart from visualizing the individual block copolymers on the mica surface, the AFM measurements provide real snapshots of the compartmentalized SCPNs before and after UV irradiation. The results further support our proposal that the triblock copolymers presented here successfully demonstrate the controlled folding of synthetic polymers into compartmentalized SCPNs via orthogonal self-assembly.

CONCLUSION

In summary, a series of ABA-type triblock copolymers with orthogonally self-assembling motifs, BTA and UPy, were readily synthesized using a postfunctionalization approach. Poly(isobornyl methacrylate) backbones having pendant alkyne and hydroxyl groups in the B and A blocks, respectively, were successfully prepared by ATRP. The resulting "bare" triblock copolymers were then functionalized using the CuAAC and isocyanate conjugation reactions, affording the triblock copolymers with distinct self-assembling motifs in a single chain. The postfunctionalization approach is broadly applicable and allows easy access to other combinations of orthogonally self-assembling moieties and polymer topologies. The triblock copolymers can thermally fold into SCPNs through intramolecular self-assembly of the BTAs to form internal columnar, helical stacks. UPy deprotection using UV light results in a further collapse of the polymers into more compact conformation via intramolecular UPy association. Well-defined single-chain nanoparticles with orthogonally self-assembling domains mimicking an α-helix and a β-sheet were successfully provided.

Our present system provides a rational design approach for self-folding protein analogues and shows the broad applicability of orthogonal self-assembly within one polymer chain as a design principle for developing synthetic enzyme mimics with well-defined tertiary folded structure. Evidently, our ability to fold synthetic macromolecules into defined, compartmentalized structures is still far from the perfection achieved in the folding of polypeptides into conformations that display selected functions. To mimic these natural systems, forming compartmentalized structures with an ordered interior is not enough. Precise location of self-assembling motifs within the polymer chain and enhanced control over polydispersities are of crucial importance for improving the scope of synthetic analogues. Recent advances in sequence-controlled polymerizations and improvements in controlled radical polymerizations will undoubtedly provide new opportunities to achieve this.[26] Currently, we are focusing on transferring the structuring concept presented in this paper to aqueous systems with the aim of making available novel enzyme mimics capable of multiple cascade reactions that show exceptionally high reactivity and selectivity for non-natural substrates. Moreover, on the basis of the present compartmentalizing technique, Janus-type SCPNs are being designed to study the self-assembly of these spherical objects.

ASSOCIATED CONTENT

Supporting Information

General information on materials and instrumentation, synthetic procedures for all block copolymers, additional CD cooling curves measured in pure DCE and 75/25 (v/v) MCH/1,4-dioxane, NMR spectra recorded during UV irradiation, SEC traces of the samples prepared at higher concentrations of 1.0 mg/mL, experimental setup and fitting analysis for SAXS data, and AFM setup and height profiles. This material is available free of charge via the Internet at http://pubs.acs.org.

AUTHOR INFORMATION

Corresponding Author

a.palmans@tue.nl; e.w.meijer@tue.nl

Notes

The authors declare no competing financial interest.

■ ACKNOWLEDGMENTS

N.H. is thankful to the Japan Society for the Promotion of Science (JSPS) for a Young Scientist Fellowship. Dr. Ilja K. Voets is acknowledged for help with interpreting SAXS data and Patrick J. M. Stals for synthesis of some compounds and help with AFM measurements. The authors express their gratitude to ESMI and the SLS for providing beam time and gratefully acknowledge the technical assistance of Dr. Andreas Menzel. The authors also thank the ICMS animation studio for the artwork. This work was supported by the European Research Council (ERC), the Dutch Science Foundation (NWO), and the National Science Foundation (DMR-1122483).

■ REFERENCES

(1) (a) Anfinsen, C. B. *Science* **1973**, *181*, 223−230. (b) Dobson, C. M. *Nature* **2003**, *426*, 884−890. (c) Lindorff-Larsen, K.; Piana, S.; Dror, R. O.; Shaw, D. E. *Science* **2011**, *334*, 517−520.

(2) (a) Cheng, R. P.; Gellman, S. H.; DeGrado, W. F. *Chem. Rev.* **2001**, *101*, 3219−3232. (b) Garcia-Viloca, M. *Science* **2004**, *303*, 186−195.

(3) Rose, G. D.; Fleming, P. J.; Banavar, J. R.; Maritan, A. *Proc. Natl. Acad. Sci. U.S.A.* **2006**, *103*, 16623−16633.

(4) (a) Whitesides, G. M.; Mathias, J. P.; Seto, C. T. *Science* **1991**, *254*, 1312−1319. (b) Rief, M.; Gautel, M.; Oesterhelt, F.; Fernandez, J. M.; Gaub, H. E. *Science* **1997**, *276*, 1109−1112. (c) Carrion-Vazquez, M.; Oberhouser, A. F.; Fowler, S. B.; Marszalek, P. E.; Broedel, S. E.; Clarke, J.; Fernandez, J. M. *Proc. Natl. Acad. Sci. U.S.A.* **1999**, *96*, 3694−3699. (d) Kushner, A. M.; Guan, Z. *Angew. Chem., Int. Ed.* **2011**, *50*, 9026−9057. (e) Whitesides, G. M.; Boncheva, M. *Proc. Natl. Acad. Sci. U.S.A.* **2002**, *99*, 4769−4774.

(5) (a) Yashima, E.; Maeda, K.; Iida, H.; Furusho, Y.; Nagai, K. *Chem. Rev.* **2009**, *109*, 6102−6211. (b) Yamamoto, T.; Yamada, T.; Nagata, Y.; Suginome, M. *J. Am. Chem. Soc.* **2010**, *132*, 7899−7901. (c) Guichard, G.; Huc, I. *Chem. Commun.* **2011**, *47*, 5933−5941.

(6) (a) Recker, J.; Tomcik, D. J.; Parquette, J. R. *J. Am. Chem. Soc.* **2000**, *122*, 10298−10307. (b) Hofacker, A. L.; Parquette, J. R. *Angew. Chem., Int. Ed.* **2005**, *44*, 1053−1057.

(7) (a) Cherian, A. E.; Sun, F. C.; Sheiko, S. S.; Coates, G. W. *J. Am. Chem. Soc.* **2007**, *129*, 11350−11351. (b) Beck, J. B.; Killops, K. L.; Kang, T.; Sivanandan, K.; Bayles, A.; Mackay, M. E.; Wooley, K. L.; Hawker, C. J. *Macromolecules* **2009**, *42*, 5629−5635. (c) Adkins, C. T.; Muchalski, H.; Harth, E. *Macromolecules* **2009**, *42*, 5786−5792. (d) Murray, B. S.; Fulton, D. A. *Macromolecules* **2011**, *44*, 7242−7252. (e) Schmidt, B. V. K. J.; Fechler, N.; Falkenhagen, J.; Lutz, J.-F. *Nat. Chem.* **2011**, *3*, 234−238. (f) Ormategui, N.; García, I.; Padro, D.; Cabañero, G.; Grande, H. J.; Loinaz, I. *Soft Matter* **2012**, *8*, 734−740. (g) Zamfir, M.; Theato, P.; Lutz, J.-F. *Polym. Chem.* **2012**, *3*, 1796−1802.

(8) (a) Seo, M.; Beck, B. J.; Paulusse, J. M. J.; Hawker, C. J.; Kim, S. Y. *Macromolecules* **2008**, *41*, 6413−6418. (b) Altintas, O.; Gerstel, P.; Dingenouts, N.; Barner-Kowollik, C. *Chem. Commun.* **2010**, *46*, 6291−6293. (c) Altintas, O.; Rudolph, T.; Barner-Kowollik, C. *J. Polym. Sci., Part A: Polym. Chem.* **2011**, *49*, 2566−2576. (d) Appel, E. A.; Dyson, J.; del Barrio, J.; Walsh, Z.; Scherman, O. A. *Angew. Chem., Int. Ed.* **2012**, *51*, 4185−4189. (e) Altintas, O.; Lejeune, E.; Gerstel, P.; Barner-Kowollik, C. *Polym. Chem.* **2012**, *3*, 640−651.

(9) For recent reviews, see: (a) Pollino, J. M.; Weck, M. *Chem. Soc. Rev.* **2005**, *34*, 193−207. (b) South, C. R.; Burd, C.; Weck, M. *Acc. Chem. Res.* **2007**, *40*, 63−74. (c) Bergman, D. S.; Wudl, F. *J. Mater. Chem.* **2008**, *18*, 41−62. (d) Aiertza, M. K.; Odriozola, I.; Cabañero, G.; Grande, H.-J.; Loinaz, I. *Cell. Mol. Life Sci.* **2012**, *69*, 337−346. (e) Ouchi, M.; Badi, N.; Lutz, J.-F.; Sawamoto, M. *Nat. Chem.* **2011**, *3*, 917−924. (f) Altintas, O.; Barner-Kowollik, C. *Macromol. Rapid Commun.* **2012**, *33*, 958−971.

(10) (a) Mes, T.; van der Weegen, R.; Palmans, A. R. A.; Meijer, E. W. *Angew. Chem., Int. Ed.* **2011**, *50*, 5085−5089. (b) Terashima, T.; Mes, T.; de Greef, T. F. A.; Gillissen, M. A. J.; Besenius, P.; Palmans, A. R. A.; Meijer, E. W. *J. Am. Chem. Soc.* **2011**, *133*, 4742−4745.

(11) (a) Foster, E. J.; Berda, E. B.; Meijer, E. W. *J. Am. Chem. Soc.* **2009**, *131*, 6964−6966. (b) Foster, E. J.; Berda, E. B.; Meijer, E. W. *J. Polym. Sci., Part A: Polym. Chem.* **2011**, *49*, 118−126. (c) Berda, E. B.; Foster, E. J.; Meijer, E. W. *Macromolecules* **2010**, *43*, 1430−1437. (d) Stals, P. J. M.; Gillissen, M. A. J.; Nicolaÿ, R.; Palmans, A. R. A.; Meijer, E. W. In preparation.

(12) (a) Ogata, D.; Shikata, T.; Hanabusa, K. *J. Phys. Chem. B* **2004**, *108*, 15503−15510. (b) Smulders, M. M. J.; Schenning, A. P. H. J.; Meijer, E. W. *J. Am. Chem. Soc.* **2008**, *130*, 606−611. (c) Stals, P. J. M.; Everts, J. C.; de Bruijn, R.; Filot, I. A. W.; Smulders, M. M. J.; Martín-Rapún, R.; Pidko, E. A.; de Greef, T. F. A.; Palmans, A. R. A.; Meijer, E. W. *Chem.—Eur. J.* **2010**, *16*, 810−821. (d) Smulders, M. M. J.; Stals, P. J. M.; Mes, T.; Paffen, T. F. E.; Schenning, A. P. H. J.; Palmans, A. R. A.; Meijer, E. W. *J. Am. Chem. Soc.* **2010**, *132*, 620−626. (e) Smulders, M. M. J.; Nieuwenhuizen, M. M. L.; Grossman, M.; Filot, I. A.; Lee, C. C.; de Greef, T. F. A.; Schenning, A. P. H. J.; Palmans, A. R. A. *Macromolecules* **2011**, *44*, 6581−6587. (f) Nakano, Y.; Hirose, T.; Stals, P. J. M.; Meijer, E. W.; Palmans, A. R. A. *Chem. Sci.* **2012**, *3*, 148−155.

(13) (a) de Greef, T. F. A.; Ercolani, G.; Ligthart, G. B. W.; Sijbesma, R. P. *J. Am. Chem. Soc.* **2008**, *130*, 13755−13764. (b) de Greef, T. F. A.; Smulders, M. M. J.; Wolffs, M.; Schenning, A. P. H. J.; Sijbesma, R. P.; Meijer, E. W. *Chem. Rev.* **2009**, *109*, 5687−5754. (c) Nieuwenhuizen, M. M. L.; de Greef, T. F. A.; van der Bruggen, R. L. J.; Paulusse, J. M. J.; Appel, W. P. J.; Smulders, M. M. J.; Sijbesma, R. P.; Meijer, E. W. *Chem.—Eur. J.* **2010**, *16*, 1601−1612. (d) de Greef, T. F. A.; Nieuwenhuizen, M. M. L.; Sijbesma, R. P.; Meijer, E. W. *J. Org. Chem.* **2010**, *75*, 598−610.

(14) (a) Brizard, A.; Stuart, M.; van Bommel, K.; Friggeri, A.; de Jong, M.; van Esch, J. *Angew. Chem., Int. Ed.* **2008**, *47*, 2063−2066. (b) Ambade, A. V.; Yang, S. K.; Weck, M. *Angew. Chem., Int. Ed.* **2009**, *48*, 2894−2898. (c) Ambade, A. V.; Burd, C.; Higley, M. N.; Nair, K. P.; Weck, M. *Chem.—Eur. J.* **2009**, *15*, 11904−11911. (d) Fox, J. D.; Rowan, S. J. *Macromolecules* **2009**, *42*, 6823−6835. (e) Yang, S. K.; Ambade, A. V.; Weck, M. *J. Am. Chem. Soc.* **2010**, *132*, 1637−1645. (f) Yang, S. K.; Ambade, A. V.; Weck, M. *Chem. Soc. Rev.* **2011**, *40*, 129−137. (g) Gröger, G.; Meyer-Zaika, W.; Böttcher, C.; Gröhn, F.; Ruthard, C.; Schmuck, C. *J. Am. Chem. Soc.* **2011**, *133*, 8961−8971. (h) Li, S.-L.; Xiao, T.; Lin, C.; Wang, L. *Chem. Soc. Rev.* **2012**, *41*, 5950−5968.

(15) (a) Mes, T.; Koenigs, M. M. E.; Scalfani, V. F.; Bailey, T. S.; Meijer, E. W.; Palmans, A. R. A. *ACS Macro Lett.* **2012**, *1*, 105−109. (b) Roosma, J.; Mes, T.; Leclére, P.; Palmans, A. R. A.; Meijer, E. W. *J. Am. Chem. Soc.* **2008**, *130*, 1120−1121. (c) Mes, T.; Smulders, M. M. J.; Palmans, A. R. A.; Meijer, E. W. *Macromolecules* **2010**, *43*, 1981−1991. (d) Appel, W. P. J.; Portale, G.; Wisse, E.; Dankers, P. Y. W.; Meijer, E. W. *Macromolecules* **2011**, *44*, 6776−6784.

(16) Barner-Kowollik, C.; Du Prez, F. E.; Espeel, P.; Hawker, C. J.; Junkers, T.; Schlaad, H.; van Camp, W. *Angew. Chem., Int. Ed.* **2010**, *50*, 60−62.

(17) (a) Patten, T. E.; Matyjaszewski, K. *Acc. Chem. Res.* **1999**, *32*, 895−903. (b) Coessens, V.; Pintauer, T.; Matyjaszewski, K. *Prog. Polym. Sci.* **2001**, *26*, 337−377. (c) Matyjaszewski, K.; Xia, J. H. *Chem. Rev.* **2001**, *101*, 2921−2990. (d) Kamigaito, M.; Ando, T.; Sawamoto, M. *Chem. Rev.* **2001**, *101*, 3689−3745.

(18) (a) Sumerlin, B. S.; Tsarevsky, N. V.; Louche, G.; Lee, R. Y.; Matyjaszewski, K. *Macromolecules* **2005**, *38*, 7540−7545. (b) Ladmiral, V.; Mantovani, G.; Clarkson, G. L.; Cauet, S.; Irwin, J. L.; Haddleton, D. M. *J. Am. Chem. Soc.* **2006**, *128*, 4823−4830.

(19) (a) Börner, H. G.; Beers, K.; Matyjaszewski, K.; Sheiko, S. S.; Möller, M. *Macromolecules* **2001**, *34*, 4375−4383. (b) Gao, H.; Matyjaszewski, K. *J. Am. Chem. Soc.* **2007**, *129*, 6633−6639. (c) Lee, H.; Pietrasik, J.; Sheiko, S. S.; Matyjaszewski, K. *Prog. Polym. Sci.* **2010**, *35*, 24−44.

(20) (a) Haddleton, D. M.; Jasieczek, C. B.; Hannon, M. J.; Shooter, A. J. *Macromolecules* **1997**, *30*, 2190−2193. (b) Haddleton, D. M.; Crossman, M. C.; Dana, B. H.; Duncalf, D. J.; Heming, A. M.; Kukulj,

D.; Shooter, A. J. *Macromolecules* **1999**, *32*, 2110−2119. (c) Darcos, V.; Haddleton, D. M. *Eur. Polym. J.* **2003**, *39*, 855−862.
(21) (a) Börner, H. G.; Duran, D.; Matyjaszewski, K.; da Silva, M.; Sheiko, S. S. *Macromolecules* **2002**, *35*, 3387−3394. (b) Lee, H.-I.; Matyjaszewski, K.; Yu, S.; Sheiko, S. S. *Macromolecules* **2005**, *38*, 8264−8271.
(22) Wegner, M.; Dudenko, D.; Sebastiani, D.; Palmans, A. R. A.; de Greef, T. F. A.; Graf, R.; Spiess, H. W. *Chem. Sci.* **2011**, *2*, 2040−2049.
(23) See the Supporting Information.
(24) de Gennes, P. *Scaling Concepts in Polymer Physics*; Cornell University Press: Ithaca, NY, 1979.
(25) (a) Percec, V.; Ahn, C.-H.; Cho, W.-D.; Jamieson, A. M.; Kim, J.; Leman, T.; Schmidt, M.; Gerle, M.; Möller, M.; Prokhorova, S. A.; Sheiko, S. S.; Cheng, S. Z. D.; Zhang, A.; Ungar, G.; Yeardley, D. J. P. *J. Am. Chem. Soc.* **1998**, *120*, 8619−8631. (b) Percec, V.; Ahn, C.-H.; Ungar, G.; Yeardley, D. J. P.; Möller, M.; Sheiko, S. S. *Nature* **1998**, *391*, 161−164. (c) Prokhorova, S. A.; Sheiko, S. S.; Möller, M.; Ahn, C.-H.; Percec, V. *Macromol. Rapid Commun.* **1998**, *19*, 359−366. (d) Percec, V.; Obata, M.; Rudick, J. G.; De, R. B.; Glodde, M.; Bera, T. K.; Magonov, S. N.; Balagurusamy, V. S. K.; Heiney, P. A. *J. Polym. Sci., Part A: Polym. Chem.* **2002**, *40*, 3509−3533. (e) Percec, V.; Glodde, M.; Bera, T. K.; Miura, Y.; Shiyanovskaya, I.; Singer, K. D.; Balagurusamy, V. S. K.; Heiney, P. A.; Schnell, I.; Rapp, A.; Spiess, H.-W.; Hudson, S. D.; Duan, H. *Nature* **2002**, *419*, 384−387. (f) Percec, V.; Rudick, J. G.; Peterca, M.; Wagner, M.; Obata, M.; Mitchell, C. M.; Cho, W.-D.; Balagurusamy, V. S. K.; Heiney, P. A. *J. Am. Chem. Soc.* **2005**, *127*, 15257−15264. (g) Rudick, J. G.; Percec, V. *Acc. Chem. Res.* **2008**, *41*, 1641−1652. (h) Rosen, B. M.; Wilson, C. J.; Wilson, D. A.; Peterca, M.; Imam, M. R.; Percec, V. *Chem. Rev.* **2009**, *109*, 6275−6540.
(26) (a) Zamfir, M.; Lutz, J.-F. *Nat. Commun.* **2012**, *3*, No. 1138. (b) Chan-Seng, D.; Zamfir, M.; Lutz, J.-F. *Angew. Chem., Int. Ed.* **2012**, 12254−12257. (c) Ouchi, M.; Terashima, T.; Sawamoto, M. *Acc. Chem. Res.* **2008**, *41*, 1120−1132.